Effect of Sequence Distribution on Copolymer Interfacial Activity

Michelle D. Lefebvre,[†] Christine M. Dettmer,[‡] Rachel L. McSwain,[†] Chen Xu,[§] Jonathan R. Davila,[‡] Russell J. Composto,[§] SonBinh T. Nguyen,[‡] and Kenneth R. Shull*,[†]

Department of Materials Science and Engineering and Department of Chemistry, Northwestern University, Evanston, Illinois 60208, and Department of Materials Science and Engineering and Laboratory for Research on the Structure of Matter, University of Pennsylvania, Philadelphia, Pennsylvania 19104-6272

Received May 10, 2005; Revised Manuscript Received September 2, 2005

ABSTRACT: Interfacial segregation of diblock, gradient, and random copolymers was measured using forward recoil spectrometry. The polymers were synthesized by a ring-opening metathesis polymerization, allowing a high degree of control over the sequence distribution. The norbornene-based monomers have reactivity ratios close to unity, which makes them ideal for facile tailoring of different gradient copolymer profiles. The copolymers form a good weakly segregating model system for which we can obtain an estimate of the interaction parameter χ. Mean-field theory was used to describe the interfacial segregation results and to relate the measured quantities to the detailed molecular structure of the interface. The diblock copolymer forms a monolayer at the interface and significantly reduces the interfacial tension, while the random copolymer forms an interfacial wetting layer. The gradient copolymer exhibits intermediate behavior, forming a monolayer with a larger interfacial width than that of the diblock copolymer.

Introduction

Recent advances in living polymerization chemistry have made possible the synthesis of a variety of new gradient copolymers where the average composition of the copolymer varies continuously along the backbone of the polymer molecule.[1−22] These gradient copolymers have properties that are intermediate between those of random copolymers, which have a uniform average composition along the contour length of the polymer molecule, and traditional block copolymers, which exhibit a step function change in composition at the junction point between the blocks. To date, gradient copolymers have been successfully synthesized by nitroxide-mediated controlled radical polymerization (NM-CRP),[3,6−10] atom-transfer radical polymerization (ATRP),[1−4,11−19] and reversible addition−fragmentation transfer polymerization (RAFT).[4,5] Recently, we reported the first synthesis of gradient copolymers by ring-opening metathesis polymerization (ROMP).[20]

Several theoretical studies have been conducted regarding the properties and applications of gradient copolymers.[23−27] The order−disorder transition and microphase separation morphology have been examined in bulk gradient copolymers,[23−25] and numerical self-consistent field theory was used to describe the equilibrium interfacial behavior of gradient copolymers in immiscible polymer blends.[26] Pickett also described how the significance of the gradient affects the density of free polymer ends at the surface of gradient copolymer brushes.[27]

While there is a growing number of reports on the synthesis of gradient copolymers, there have been few experimental studies that report on their properties.[3,4,6,8,9,12,13,28] Many of these studies have resulted in data that indicate similarity between gradient copolymers and either their random or block copolymer counterparts. Farcet and Charleux detected only one glass transition in their styrene/*n*-butyl acrylate copolymers with weak gradients.[6] Matyjaszewski et al. demonstrated microphase separation of copolymers with a much stronger gradient through both thermal and rheological analysis for styrene/methyl acrylate gradient copolymers[12] and by small-angle X-ray scattering (SAXS) in styrene/acrylonitrile gradient copolymers.[13] They observed a single glass transition in a thermally quenched gradient copolymer and two glass transitions in an annealed gradient copolymer. Gray and co-workers observed differences in the enthaply recovery behavior of styrene/4-methylstyrene[9] gradient and styrene/4-acetoxystyrene[8] "blocky" gradient copolymers in comparison to their random counterparts. Recently, Kim and co-workers demonstrated the compatibilization potential of gradient copolymers in melt-processed blends.[28] They observed that a gradient copolymer significantly stabilized immiscible blends and reduced coarsening. Using only 5% gradient copolymer, coalescence was prevented in a styrene/methyl methacrylate system and was significantly reduced in the more incompatible styrene/*n*-butyl methacrylate system.

Studies of the segregation of gradient copolymers to the interface between immiscible homopolymers are particularly important, both in the development of new routes for polymer blend compatibilization and in the development of a robust theory for the thermodynamic properties of gradient copolymer systems. Polymer blends are important for the development of new materials, but most polymer blends are incompatible and result in poor morphology, weak adhesion between phases, high interfacial tension, loss of mechanical properties, and coalescence and breakup during processing. Copolymers added as compatibilizers act as surfactants by localizing at the interface, lowering the interfacial tension, and dividing the immiscible poly-

[†] Department of Materials Science and Engineering, Northwestern University.
[‡] Department of Chemistry, Northwestern University.
[§] University of Pennsylvania.
* To whom correspondence should be addressed: e-mail k-shull@northwestern.edu.

10.1021/ma0509762 CCC: $30.25
Published on Web 11/10/2005

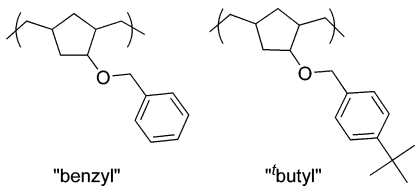

Figure 1. Repeat units of the two homopolymers.

mers into smaller domains. In an AB block compatibilizer, the A block inserts into the A homopolymer domain and the B block inserts into the B homopolymer domain.[29] Theoretical studies have shown that random copolymers will weave in and out of the interface, forming loops in each homopolymer domain.[30,31] These entanglements strengthen the interface by "tying" the phases together, but a single copolymer monolayer is not obtained; instead, a third phase or wetting layer is observed, which limits compatibilization.[32−34]

It has been suggested that long block copolymers compatibilize better than random copolymers,[35] but in practice they can form micelles at low concentrations so that individual molecules do not diffuse to the interface.[36,37] Mean-field theory has been remarkably successful in providing a quantitative description of the surfactant-like monolayer that is formed at the interface by traditional block copolymers and of the limitations associated with micellization.[35,38,39] Imposition of an increasingly broad composition gradient in the copolymer broadens the width over which different segment types mix with one another while preserving the monolayer-like character of the copolymer layer.[26] Mean-field theory predicts that the interfacial width depends on the gradient copolymer's radius of gyration and the nature of the composition gradient. The critical micelle concentration was also calculated to be larger for gradient copolymers than block copolymers, meaning gradient copolymers would be more likely to diffuse to the interface and improve blend quality.

Previous studies on sequence distributions in copolymers have focused on random copolymers. Fredrickson, Milner, and Leibler[40] as well as Shakhnovich and co-workers[41,42] have developed theories to describe random copolymers and the relationship between microphase separation and the "blockiness" of the polymer. Balazs and co-workers accounted for random copolymer sequence distributions explicitly in mean-field calculations and found that the best random copolymer compatibilizers have composition distributions very closely centered around 50%.[35,43] In this article we focus on an ideal random copolymer with a uniform composition profile and compare it to gradient and diblock copolymers. Random and gradient copolymers are inherently different from diblock copolymers because they are statistical copolymers. While the sequence distribution for a diblock copolymer is the same for every molecule, each random and gradient copolymer molecule is different. We describe a set of model experiments aimed at studying the effect of sequence distribution on the interfacial segregation of copolymer molecules.

The model system we utilize consists of norbornene-based polymers synthesized using ring-opening metathesis polymerization (ROMP). ROMP is advantageous in that it allows for polymerization at room temperature with much faster rates of reaction than living free radical approaches.[20] Three copolymers and two homopolymers were synthesized using the repeat units shown in Figure 1: "benzyl" (homopolymer glass transition temperature T_g = 6.4 °C) and "^{t}butyl" (T_g = 36.4 °C).[20] The corresponding monomers, **1a** and **1b**, are shown in Scheme 1. A deuterated version of the benzyl monomer, **2**, was synthesized and used in the copolymer synthesis so that the copolymers could be detected using forward recoil spectrometry (FRES). Interfacial segregation of the copolymers to an interface between the two immiscible homopolymers was measured using FRES, and mean-field theory was used to fit the data and calculate the interfacial excess, interfacial tension, and degree of incompatibility for each sample.

Scheme 1. Synthesis of 1a and 1b

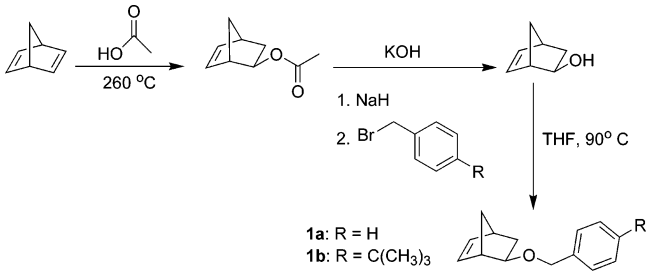

Experimental Section

Materials. HPLC-grade tetrahydrofuran (THF) was purified using the Dow-Grubbs purification system,[44] collected under argon, degassed under vacuum, and stored under nitrogen in a Strauss flask prior to use. Ethyl vinyl ether was dried over CaH_2, vacuum-transferred into an airtight solvent bulb prior to transfer into an inert-atmosphere glovebox, and stored at 0 °C. All monomers were synthesized and stored under nitrogen at 0 °C. Deuterated solvents (Cambridge Isotope Laboratories) and all other solvents and reagents were purchased from commercial sources and used without further purification.

Methods. All reactions were carried out under a dry nitrogen atmosphere using standard Schlenk techniques or in an inert-atmosphere glovebox, unless otherwise noted. Conversion of the copolymerizations was determined on a Hewlett-Packard 5890A gas chromatograph equipped with a FID detector and a 30 m HP-5 capillary column (0.32 mm inner diameter, 0.25 mm film thickness; method: initial time = 0 min, initial temp = 50 °C, rate = 10 °C/min, final temp = 250 °C, final time = 5 min) using undecane as an internal standard. Molecular weights relative to polystyrene standards were measured on a Waters gel-permeation chromatograph (GPC) equipped with Breeze software, a 717 autosampler, Shodex KF-G guard column, KF-803L and KF-806L columns in series, a Waters 2440 UV detector, and a 410 RI detector. HPLC-grade THF was used as the eluent at a flow rate of 1.0 mL/min, and the instrument was calibrated using polystyrene standards (Aldrich, 15 standards, 760−1 800 000 Da). ^{1}H NMR spectra were recorded on a Varian Mercury 400 FT-NMR spectrometer (400.178 MHz for ^{1}H). ^{13}C NMR spectra were recorded on a Varian Inova 500 FT-NMR spectrometer (125.669 MHz for ^{13}C). ^{1}H NMR data are reported as follows: chemical shift (multiplicity: br = broad, s = singlet, d = doublet, t = triplet, q = quartet, and m = multiplet), peak assignments, and integration. ^{1}H and ^{13}C chemical shifts are reported in ppm downfield from tetramethylsilane (TMS, δ scale) with the residual solvent resonances as internal standards, while peak assignments were made using ACD/Labs software packages (Advanced Chemistry Development, Inc.). GC-MS experiments were recorded on a Hewlett-Packard 6890 series instrument equipped with a HP-5 column (initial time = 2 min, initial temp = 50 °C, rate = 10 °C/min, final temp = 280 °C, final time = 5 min). All flash column chromatography was performed under a positive pressure of nitrogen using 230−400 mesh silica gel (56 mm i.d. × 200 mm L), unless otherwise noted. Monomer addition was carried out via either a Kd

Scientific KDS200 syringe pump or a Harvard Apparatus syringe pump model 55-1111.

***exo*-5-(Benzyloxy)norbornene (1a)** was prepared as reported previously.[20]

***exo*-5-[(4-^{t}Butyl)benzyloxy]norbornene (1b)** was prepared as reported previously.[20]

Benzyl-d_7 bromide was prepared from standard literature procedures.[45,46] The crude product was purified by flash column chromatography with 20:80 methylene chloride:hexanes as the elutant.

***exo*-5-(Benzyloxy)norbornene-d_7 (2)** was prepared by the same procedure used to prepare **1a** and **1b**. A colorless oil was obtained (5.1813 g, 82.8%) ^{1}H NMR ($CDCl_3$): δ 1.58 (m, 7-norbornenyl-H_2, 2H), 1.78 (d, 6-norbornenyl-H_2, 2H), 2.84 (s, 4-norbornenyl-*H*, 1H), 2.97 (s, 1-norbornenyl-*H*, 1H), 3.62 (d, 5-norbornenyl-*H*, 1H), 5.95 (m, 3-norbornenyl-*H*, 1H), 6.21 (m, 2-norbornenyl-*H*, 1H). ^{13}C NMR ($CDCl_3$): δ 34.7 (6-norbornenyl-*C*), 40.6 (1-norbornenyl-*C*), 46.3 (7-norbornenyl-*C*), 46.7 (4-norbornenyl-*C*), 70.4 (m, benzyl-*C*, J = 87.2 Hz), 80.2 (5-norbornenyl-*C*), 126.9 (m, *p*-aromatics-*C*, J = 97.5 Hz), 127.2 (m, *m*-aromatics-*2C*, J = 96.5 Hz) 127.8 (m, *o*-aromatics-*2C*, J = 96.5 Hz), 133.4 (3-norbornenyl-*C*), 138.9 (*ipso*-*C*), 140.92 (2-norbornenyl-*C*). EIMS: calcd for $C_{14}H_9D_7O$: 207.32; found: 207.2.

Synthesis of Homopolymers of 1a and 1b. In a typical polymerization, a scintillation vial equipped with a stir bar was charged with either **1a** or **1b** (4.9 mmol) and diluted with THF (10 mL). Another scintillation vial was charged with Grubbs catalyst **3** (8.0 mg, 9.7×10^{-3} mmol) and diluted with THF (1 mL). The catalyst solution was injected into the stirring monomer solution, and the vial was capped. The vial was removed from the glovebox, and after 40 min the polymerization was quenched with ethyl vinyl ether (2 mL). 2,6-Di-*tert*-butyl-4-methylphenol (BHT) (30 mg) was added, and the polymer was precipitated in swirling methanol. The final polymer was dried for 2 days under vacuum.

Synthesis of Asymmetrical Block Copolymer of 2 and 1b. A scintillation vial equipped with a stir bar was charged with **2** (500.9 mg, 2.420 mmol) and diluted with THF (7 mL). Another scintillation vial was charged with Grubbs catalyst **3** (2.5 mg, 3.0×10^{-3} mmol) and diluted with THF (1 mL). The catalyst solution was injected into the stirring monomer solution, and the vial was capped. Another scintillation vial was charged with **1b** (145.4 mg, 5.67×10^{-1} mmol) and diluted with THF (2 mL). After 40 min of polymerization, the **1b** solution was injected into the reaction mixture. The vial was rinsed with THF (1 mL × 3) and added to the reaction mixture. The reaction vial was removed from the glovebox, and after 40 min the polymerization was quenched with ethyl vinyl ether (2 mL). BHT (30 mg) was added, and the polymer was precipitated in swirling methanol. The final polymer was dried for 2 days under vacuum.

Synthesis of Random Copolymers of 2 and 1b. A scintillation vial equipped with a stir bar was charged with **2** (459.6 mg, 2.220 mmol) and **1b** (571.0 mg, 2.230 mmol) and diluted with THF (15 mL). Another scintillation vial was charged with Grubbs catalyst **3** (7.5 mg, 9.1×10^{-3} mmol) and diluted with THF (1 mL). The catalyst solution was injected into the stirring monomer solution, and the vial was capped. The vial was removed from the glovebox, and after 40 min the polymerization was quenched with ethyl vinyl ether (2 mL). BHT (30 mg) was added, and the polymer was precipitated in swirling methanol. The final polymer was dried for 2 days under vacuum.

Synthesis of Gradient Copolymers, Dual Ramping. In an inert-atmosphere glovebox, two 10 mL volumetric flaks were charged with monomer **2** (0.8699 g, 4.202 mmol) and **1b** (0.6508 g, 2.542 mmol), respectively, and diluted with THF. Both solutions were taken up into 10 mL gastight syringes and then plugged with a septa. In a 20 mL vial, Grubbs catalyst **3** (8.3 mg, 1.0×10^{-1} mmol) was dissolved in THF (2 mL), loaded into a 2.5 mL gastight syringe, and plugged with a septa.

Next, a 500 mL round-bottom flask equipped with a magnetic stir bar was charged with **2** (4 μL, 2.4×10^{-2} mmol), **1b** (100 μL, 3.89×10^{-1} mmol), undecane (100 μL, 4.75×10^{-1} mmol), and THF (140 mL) and capped with a rubber setpum. The syringes and the flask were removed from the glovebox. Outside the glovebox, the syringes were loaded onto two different syringe pumps and immediately attached to the flask by removing their septa and inserting the needles through the flask's septum while the flask was allowed to stir rapidly. The catalyst solution was injected into the reaction flask, and the solutions of **2** and **1b** were simultaneously added via the syringe pumps. The addition rate of the **2** solution was ramped up while the **1b** solution was ramped down every 3−6 min (Table 1). Disposable syringes and needles used to remove aliquots were purged with nitrogen before use. Aliquots (2 mL) were taken 1 min after each change in addition rate and quenched with ethyl vinyl ether (1 mL).[47] BHT (5 mg) and triphenylphosphine oxide (20 mg) were then added to each aliquot. A portion of each aliquot (0.3 mL) was loaded on a plug of silica gel (3.55 cm L × 0.55 cm i.d.), eluted with CH_2Cl_2 (8 mL) and was analyzed by GC. The amount of monomer incorporated into the polymer was calculated from the amount of remaining monomer. The remaining portion of each aliquot was concentrated on a rotary evaporator to about 0.1 mL. Methanol (2 mL) was then added to the residue to precipitate the polymer, the mother liquor was decanted, and the polymer was dried under vacuum overnight before being analyzed by GPC.

Table 1. Monomer Addition Rates (mmol/h) of 2 and 1b throughout the Reaction for Dual-Ramping Polymerization

	time (min)							
monomer	0	3	6	12	18	24	30	36
2	1.3	2.0	2.8	3.3	3.8	5.8	9.1	12.6
1b	10.4	7.6	5.1	3.6	2.0	1.8	1.0	0.0

The reaction was quenched after 42 min with ethyl vinyl ether (5 mL). BHT (200 mg) and triphenylphosphine oxide (300 mg) were then added to the flask. The reaction solution was concentrated on a rotary evaporator to about 5 mL and precipitated in rapidly stirred methanol (250 mL). The precipitated polymer was collected and precipitated a second time if necessary. The final polymer sample was collected and dried under vacuum before analysis by GPC.

Polymer Hydrogenation. This experiment was a modification of a literature procedure.[48] For a typical hydrogenation, in an inert nitrogen atmosphere glovebox, the ROMP polymer (1046.5 mg) was dissolved in methylene chloride (25 mL) and loaded into a 125 mL Parr reactor equipped with a magnetic stir bar. To this solution, methanol (8 mL) was slowly added. (If the polymer solution became cloudy, addition was ceased early and additional methylene chloride was added until the solution became clear again.) Grubbs catalyst **3** (22.2 mg, 27.0 mmol) was dissolved in methylene chloride (2 mL) in a scintillation vial. The Grubbs catalyst **3** solution was then added to the Parr reactor, and the vial was rinsed with methylene chloride (1.6 mL × 3). NEt_3 (15 μL) was added via a gastight syringe, and the reactor was immediately sealed, removed from the glovebox, pressurized with hydrogen (300 psig), and allowed to stir for 48 h in a 60 °C oil bath. The reaction was monitored by ^{1}H NMR spectroscopy though opening the Parr reactor in the glovebox, removing an aliquot, and precipitating the polymer. If the reaction was not complete, the Parr reactor was repressurized with H_2 and the reaction was allowed to continue. Once hydrogenation was complete, the reaction was transferred into a 500 mL round-bottom flask and the reactor was rinsed with methylene chloride (3 × 2 mL). The combined organics were concentrated on a rotary evaporator to 5 mL and precipitated into rapidly stirred methanol (200 mL). The precipitated polymer was collected, dissolved, and precipitated a second time. The final polymer sample was collected and dried under vacuum before analysis by GPC. GPC analysis was performed on both the hydrogenated and original polymer to verify that no degradation of the polymer had occurred.

Scheme 2. Synthesis of 2

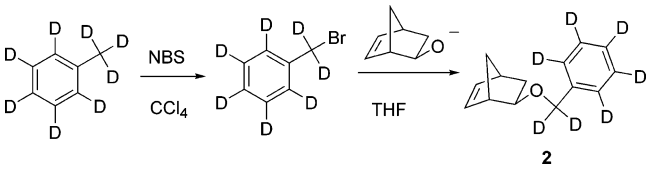

Scheme 3. General Reaction for Polymerization of Monomers and Subsequent Hydrogenation[a]

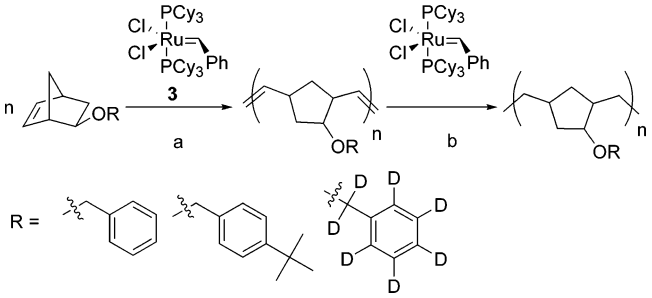

[a] (a) THF; (b) 2:8 methanol:methylene chloride, 0.5 mol % Grubbs catalyst, 5 equiv of NEt_3, 300 psig of H_2, 60 °C, 2 days.

Sample Preparation. Samples were made for FRES by layering the polymers on a silicon substrate. The benzyl homopolymer has a T_g below room temperature; therefore, it was chosen as the bottom layer for the samples. For each sample, the benzyl homopolymer was blended in a toluene solution with one of the copolymers at 5, 10, 20, or 30% copolymer and was then spun-coat from the solution onto a silicon wafer. The *t*butyl homopolymer was spun-coat from a toluene solution onto a salt crystal, floated onto water, and picked up by the benzyl homopolymer on silicon. The benzyl/copolymer layer was 600 nm thick and the *t*butyl layer was 165 nm thick, as measured by profilometry of test samples with a Tencor P-10 profilometer.

FRES. The parameters used for the FRES tests were a beam energy of 2.6 MeV and an 8 μm filter of Mylar, which correspond to a depth resolution of 50 nm and an accessible depth of 600 nm. The FRES spectra were converted to volume fraction depth profiles using deuterated standards and measured values of the relevant stopping cross sections according to the calculations presented in the review article by Composto, Walters, and Genzer.[49]

Results and Discussion

Synthesis. Monomers *exo*-5-(benzyloxy)norbornene (**1a**) and *exo*-5-[(4-*t*butyl)benzyloxy]norbornene (**1b**) were synthesized in three steps from norbornadiene (Scheme 1), as described previously.[20] The deuterated version of **1a**, monomer **2**, was synthesized by the same procedure from benzyl-d_7 bromide and norbornenol (Scheme 2). Benzyl-d_7 bromide, while commercially available, was easily synthesized through bromination of toluene-d_8. We previously demonstrated the living nature of catalyst **3** toward the ROM polymerization of **1a** and **1b** for the formation of "controlled" copolymers with linear increases in M_n over time and consistently low PDI's (Scheme 3a).

The reactivity ratios for **1a** and **1b** via ROMP using catalyst **3** were previously measured to be 0.99 ± 0.06 and 1.13 ± 0.09, respectively.[20] To form a gradient copolymer from **1b** and **2** with a significant change in chain composition, a semibatch method is used. Previous mean-field calculations predict that a symmetrical, fully tapered gradient copolymer results in a large increase in interfacial width between two immiscible homopolymers.[26] Therefore, to begin an experimental investigation into the interfacial behavior of gradient copolymers

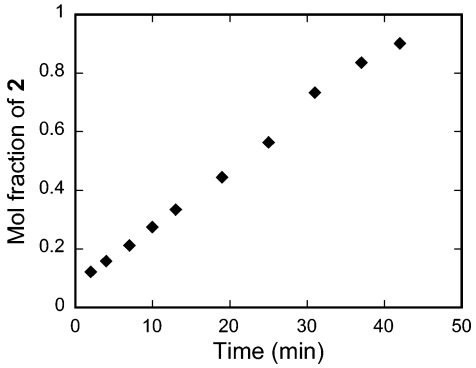

Figure 2. Linear change in the fraction of monomer **2** in the feed during the polymerization time span for the synthesis of the gradient copolymer via the dual ramping method.

in comparison to its random and block copolymer counterparts, a gradient copolymer with a linear change in chain composition and an overall monomer composition of 50% was desired. We previously described a dual ramping method to synthesize 50/50 linear gradient copolymers from monomers with reactivity ratios near unity.[20] The dual ramping method allows for more precise control of the feed ratio than continuous addition of one monomer at a set rate by changing the addition rate of both monomers in a semicontinuous fashion. This process forces the fraction of monomer in the feed to change linearly in relation to the polymerization time span, as shown in Figure 2.

For ease of experiment, we determined the extent of polymerization and monomer incorporation via GC quantification of unreacted monomer, an indirect but facile method. However, the percentage of monomer incorporated into the copolymer can also be followed by ^{1}H NMR spectroscopy at long reaction times when sufficient amounts of polymer can be recovered for analysis. From the monomer conversion data, cumulative (F_{cum}) and instantaneous compositions (F_{inst})[1] were calculated from eqs 1 and 2, where X and Y are the quantities (mol) of monomers x and y in the polymer, respectively, and ρ is conversion.

$$F_{cum} = \frac{X}{X+Y} \tag{1}$$

$$F_{inst} = F_{cum} + \rho \frac{\Delta F_{cum}}{\Delta \rho} \tag{2}$$

Figure 3 shows F_{cum} and F_{inst} of monomer **2** in the gradient copolymer synthesized via the dual ramping method as a function of normalized chain length (n/N_c). Because the reactivity ratios of the two monomers are very close to unity, the instantaneous composition (F_{inst}) is expected to track with the fraction of monomer **2** in the feed monomer, shown in Figure 2. Figure 3 shows that the polymer does have a linear gradient with an overall composition of 50% **2**, as desired.

To allow the copolymer chains to reach equilibrium in the thin film samples, long anneal times at temperatures 100−120 °C above the T_g of **1b** were required. To prevent cross-linking during the annealing, the polymers were hydrogenated (Scheme 3b) by a procedure reported by Dourin et al.[48] This procedure hydrogenates ROMP polymers efficiently at moderate hydrogen pressures with the same catalyst **3** and avoids the thermal degradation and loss of the benzyl ether that results from other common polymer hydrogenation

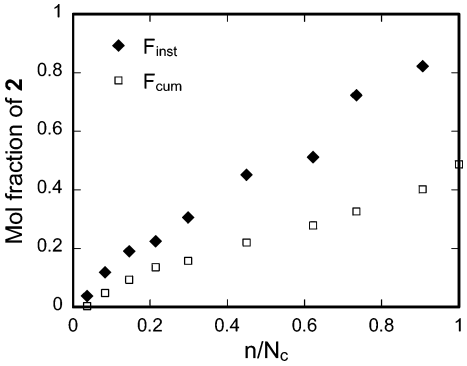

Figure 3. Change in instantaneous (F_{inst}) and cumulative (F_{cum}) composition as a function of normalized chain length for the gradient copolymer synthesized via the dual ramping method.

Table 2. Molecular Weight and Composition of ROMP Polymers

polymer	M_w (g/mol)	N_c[a]	PDI	fraction **1b**[b] ($1 - F_{cum}$)
hydrogenated poly(**1a**)	161 000	700	1.12	0
hydrogenated poly(**1b**)	128 000	555	1.16	1
hydrogenated asymmetrical block poly(**2**-*b*-**1b**)	251 000	1090	1.20	0.18
hydrogenated random poly(**2**-*r*-**1b**)	155 000	675	1.14	0.49
hydrogenated gradient poly(**2**-*g*-**1b**)	166 000	720	1.17	0.48

[a] Based on repeat unit molecular weight of 230 g/mol. [b] Determined by NMR.

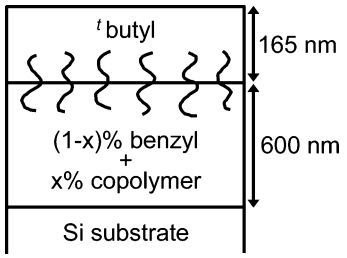

Figure 4. Sample geometry for FRES experiments. Copolymers are initially blended with benzyl homopolymer with x = 5, 10, 20, and 30% and segregate to the interface upon annealing.

methods.[20] The molecular weights and final compositions of the polymers are listed in Table 2.

Interfacial Segregation. Samples for FRES were prepared by blending each of the three deuterated copolymers with the benzyl homopolymer at 5, 10, 20, and 30% and creating a layered sample, as shown in Figure 4. Each sample was then annealed at 140 °C for 41 and 89 h and analyzed with FRES to examine the effects of initial concentration and annealing time on the interfacial segregation of the copolymer. The FRES spectra were converted to copolymer volume fraction profiles as functions of depth into the sample using deuterated standards and measured values of the relevant stopping cross sections.[49]

Diblock Copolymer. Volume fraction profiles for the asymmetric diblock copolymer at 5, 10, and 20% initial copolymer concentration are shown in Figure 5. The diblock copolymer behaves as expected, with an excess of copolymer at the interface between the homopolymers and equilibrium concentrations in each homopolymer phase. The solid line in the figure is a fit to the data using mean-field theory. The instrumental resolution of the FRES technique has been accounted for by

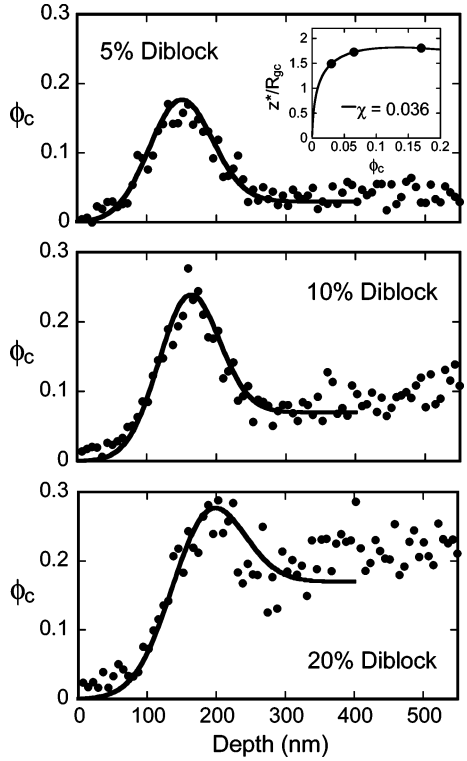

Figure 5. FRES volume fraction profiles (circles) and mean-field theory fits (lines) for diblock copolymer samples annealed for 89 h at 140 °C. The fits are calculated using $\chi = 0.036$, or $(1 - f)\chi N_c = 7.1$, which was determined by the adsorption isotherm shown in the inset.

convolving the profiles predicted by mean-field theory with a Gaussian broadening function with a full width at half-maximum of 100 nm. In this theoretical treatment of the interfacial copolymer behavior, we use "A" to denote the benzyl repeat units and "B" to denote the ^{t}butyl repeat units. We consider a model where an AB copolymer segregates to a flat interface between A and B homopolymer phases. The three copolymers—diblock, gradient, and random—are defined by their composition profiles along the chain backbone using the function $g(n)$, the average volume fraction of A at repeat unit n in a chain of N_c repeat units. The overall composition of the polymer, f, is defined as the average value of g:

$$f = \frac{1}{N_c}\int_0^{N_c} g(n)\,\mathrm{d}n = \int_0^1 g(n')\,\mathrm{d}n' \qquad (3)$$

with $n' \equiv n/N_c$. If the two repeat units have the same volume, the volume fractions f and g are equal to the mol fractions F_{cum} and F_{inst}, respectively, and eq 3 is an integral representation of eq 2. We choose a reference volume v_0 that is the same for each repeat unit and corresponds to the average repeat unit molecular weight (230 g/mol) and make the approximations that $f = F_{cum}$ and $g = F_{inst}$. We use $(1 - f)$ to describe the interactions in this system because the B block of the copolymer is the incompatible block in the initial sample geometry. An additional parameter, λ, is used to describe the fractional length of the gradient along the chain backbone.[25,26] The gradient copolymer used here has $(1 - f) = 0.5$ and a linear gradient profile that extends the entire length of the chain, i.e., $\lambda = 1$ (Figure 3). The diblock copolymer has $(1 - f) = 0.2$ and a step function concentration profile, $\lambda = 0$, and the random copolymer has $(1 - f) = 0.5$ and a uniform composition profile for which λ is infinite.

The theoretical description of the copolymer interactions begins with the Flory−Huggins expression for the free energy of the system. The free energy per unit volume, Δf, is given by the following expression

$$\Delta f = \frac{k_B T}{v_0}\left\{\frac{\phi_{ha}\ln\phi_{ha}}{N_{ha}} + \frac{\phi_{hb}\ln\phi_{hb}}{N_{hb}} + \frac{\phi_c\ln\phi_c}{N_c} + \chi\sum_k \phi_k(g_k - \phi_a)^2\right\} \quad (4)$$

where N_{ha}, N_{hb}, ϕ_{ha}, and ϕ_{hb} are the degrees of polymerization and volume fractions of A and B homopolymers, and N_c and ϕ_c are the degree of polymerization and volume fraction of the AB copolymer. The subscript k denotes each component in the system (ha, hb, or c), and the volume fraction ϕ_a refers to the total volume fraction of A repeat units. The degrees of polymerization are the weight-average molecular weights as determined by GPC, normalized by the reference volume v_0. The interaction parameter χ is defined in terms of the same reference volume.

The expression for the chemical potentials of the components, μ_k, is derived from the free energy. For a homogeneous mixture, it can be written as

$$\frac{\mu_k}{k_B T} = \frac{\ln\phi_k + 1}{N_k} - \sum_k \frac{\phi_k}{N_k} + \chi\int_0^{N_k}(g_k(n) - \phi_a)^2\,dn \quad (5)$$

The first two terms represent the ideal entropy of mixing, and the third term is the enthalpic contribution. It includes the function $g(n)$ to account for the specific composition distribution of each polymer.[26] Equilibrium is obtained when the chemical potential of each component is uniform throughout the entire system. To determine the volume fraction profiles that satisfy this condition for a multiphase system, a set of mean-field equations is solved self-consistently using an expression for the mean field that is based on the chemical potential.[38,50]

The measurable interfacial quantity that is calculated from the results is the interfacial excess, z^*. It is defined as the excess volume fraction of copolymer at the interface with respect to the volume fraction of copolymer in the bulk and is often normalized by the copolymer radius of gyration, $R_{gc} = a\sqrt{N_c/6}$, where a is the statistical segment length. We assume a value for a that results in an R_{gc} equivalent to the R_g of a polystyrene molecule of the same molecular weight.

$$z^* = \int_{-\infty}^{\infty}(\phi_c(z) - \phi_c^{bulk})\,dz \quad (6)$$

The set of mean-field equations is solved using boundary conditions corresponding to the depleted concentration of copolymer in the benzyl phase from the FRES results. The value of χ is a variable parameter that can be changed to obtain a good theoretical fit to the experimental volume fraction profile. We report our results in terms of $(1 - f)\chi N_c$ because it is a more appropriate measure of incompatibility for copolymers than χ or χN_c alone due to the uncertainty in the value of N obtained by GPC. For reference, the critical point for microphase separation in diblock copolymer melts is $(1 - f)\chi N_c = 5.25$ and increases with λ.[25] After annealing the diblock copolymer samples for 89 h at 140 °C, there is very little change in the composition profiles from samples annealed for 41 h, indicating that the samples have reached equilibrium. The mean-field theory fits show $\chi = 0.036$, or $(1 - f)\chi N_c = 7.1$, for the diblock copolymer samples with 5, 10, and 20% initial concentration of copolymer. The adsorption isotherm, the interfacial excess as a function of the depleted concentration of copolymer, for this value of χ is shown in the inset in Figure 5 with data points for the three samples. Based on the mean-field theory, the value of χ would need to be about 35% larger for micelles to form, demonstrating that the diblock copolymers diffuse to the interface without forming micelles in the benzyl phase. These results are based on an assumed degree of polymerization calculated from the chromatographically determined weight-average molecular weight. Using the number-average molecular weight to calculate N_c results in only a small change, $\chi = 0.043$, and there is not an appreciable difference in the remaining results presented.

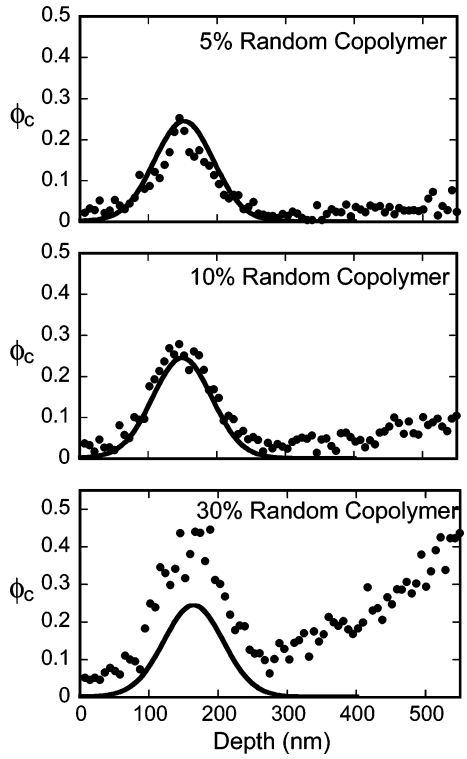

Figure 6. FRES volume fraction profiles (circles) and mean-field theory fits (lines) for random copolymer samples annealed for 89 h at 140 °C. The fits are calculated using $\chi = 0.036$, or $(1 - f)\chi N_c = 11.9$, at the coexistence chemical potential, $\mu_{coex} = -0.002$, with $z^*/R_{gc} = 2.6$.

Random Copolymer. Volume fraction profiles for the symmetric random copolymer at 5, 10, and 30% initial copolymer concentration are shown in Figure 6. While the 5% sample has a low copolymer content and has reached equilibrium, the 10 and 30% random copolymer samples, unlike the diblock copolymer, have not yet reached equilibrium. In the high copolymer content samples, there is still an excess of copolymer near the sample substrate. The random copolymers have a slow equilibration time because the random copolymer is not completely soluble in the benzyl homopolymer matrix phase. While the diblock copolymer contains only 20% of the incompatible ^{t}butyl component, the random and gradient copolymers are 50% ^{t}butyl, and are thus more incompatible with the benzyl homopolymer. Macrophase separation between a random copolymer with

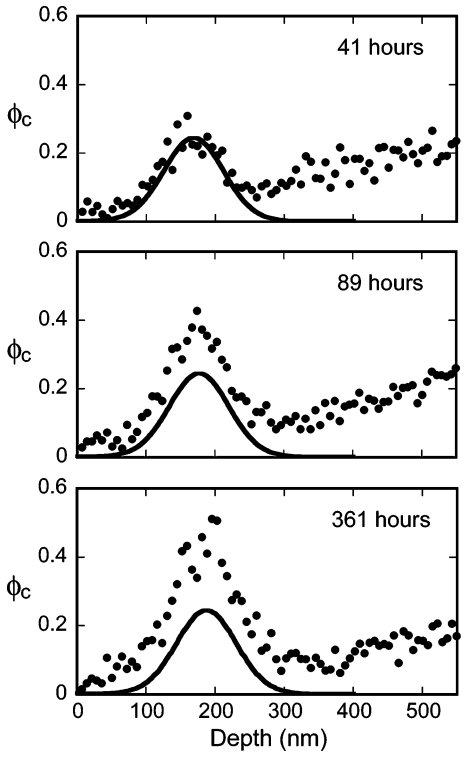

Figure 7. FRES volume fraction profiles (circles) and mean-field theory fits (lines) for 20% initial concentration random copolymer samples annealed for 41, 89, and 361 h at 140 °C. The fits are calculated using $\chi = 0.036$, or $(1 - f)\chi N_c = 11.9$, at the coexistence chemical potential, $\mu_{coex} = -0.002$, with $z^*/R_{gc} = 2.6$.

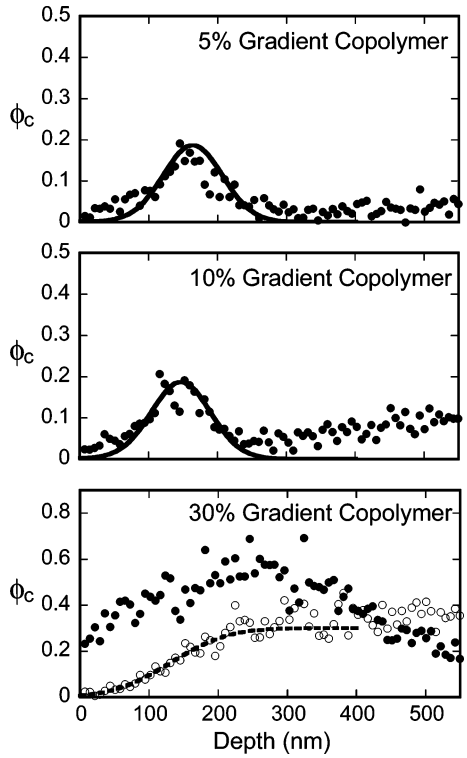

Figure 8. FRES volume fraction profiles (closed circles) and mean-field theory fits (lines) for gradient copolymer samples annealed for 89 h at 140 °C. The fits are calculated using $\chi = 0.036$, or $(1 - f)\chi N_c = 12.5$, at the coexistence chemical potential, $\mu_{coex} = 2.16$, with $z^*/R_{gc} = 1.9$. The open circles show the unannealed volume fraction profile for 30% initial concentration for comparison.

$f = 0.5$ and a homopolymer of equal length occurs at $(1 - f)\chi N_c = 4$. Using the value of χ determined by the diblock copolymer samples, $\chi = 0.036$, this random copolymer has $(1 - f)\chi N_c = 11.9$, which is well above the phase separation limit. In fact, the random copolymer has a calculated maximum solubility of 0.24% in the benzyl homopolymer, and it undergoes phase separation to form domains of a second, copolymer-rich phase within this layer.

Additional tests were performed on the random copolymer samples at a very long annealing time of 361 h. Figure 7 shows the volume fraction profiles after 41, 89, and 361 h for the 20% initial concentration sample. After 361 h, the sample has still not reached equilibrium. Because the copolymer and homopolymer are phase-separated, there can only be 0.24% of solubilized copolymer in the benzyl phase, and thus only a very small fraction of copolymer can be diffusing toward the interface at a given time. Thus, the remaining copolymer is "tied up" in the copolymer-rich domains, and the sample has a very slow equilibration time.

Gradient Copolymer. Volume fraction profiles for the symmetric gradient copolymer at 5, 20, and 30% initial copolymer concentration are shown in Figure 8. Like the random copolymer, the gradient copolymer has low solubility in the benzyl homopolymer matrix. At $\chi = 0.036$, the gradient copolymer has $(1 - f)\chi N_c = 12.5$ and a maximum solubility of 0.15% in the benzyl homopolymer. Thus, the gradient copolymer phase separates to form copolymer-rich domains in the benzyl layer, and the 10% sample has not yet reached equilibrium after 89 h of annealing. The 5% sample has a low enough copolymer content so that all of the copolymer has reached the interface, similar to the results for the random copolymer. The 30% initial concentration sample exhibits a different behavior, with a moderate volume fraction of gradient copolymer throughout the sample after annealing. As discussed below, this result is suggestive of the formation of an emulsion phase at the interface, but the FRES data do not give us enough information to determine the structure of this sample.

Interface Character. Mean-field fits to the data are shown as the solid lines in Figures 6−8 at the solubility limits for the respective copolymers. For the random copolymer, this occurs at a copolymer coexistence chemical potential, μ_{coex}, of −0.002, with $z^*/R_{gc} = 2.6$. For the gradient copolymer, coexistence is at $\mu_{coex} = 2.16$ with $z^*/R_{gc} = 1.9$. At low initial concentrations of copolymer, 5 and 10%, the calculated volume fraction profiles fit the experimental data well for both of the statistical copolymers. However, at high concentrations of random copolymer, 20 and 30%, the experimental interfacial excess is 2−2.5 times larger than the predicted value at coexistence. This is because the random copolymer molecules have small variations in chemical composition and molecular weight among themselves. While the mean-field theory assumes that every chain is the same and has an average composition of 50%, the actual random copolymer molecules will differ from each other, with some having a higher interfacial activity.[35,43,51−54] For an ideal random copolymer, the chemical composition portion of a Stockmayer distribution[55,56] suggests that about 5% of the molecules will differ in composition from the mean by more than 4%. Assuming a Gaussian distribution in molecular weight and a polydispersity index of 1.14, 10% of the molecules will have a molecular weight more than 1.5 times greater than the mean. These differences within the population of random

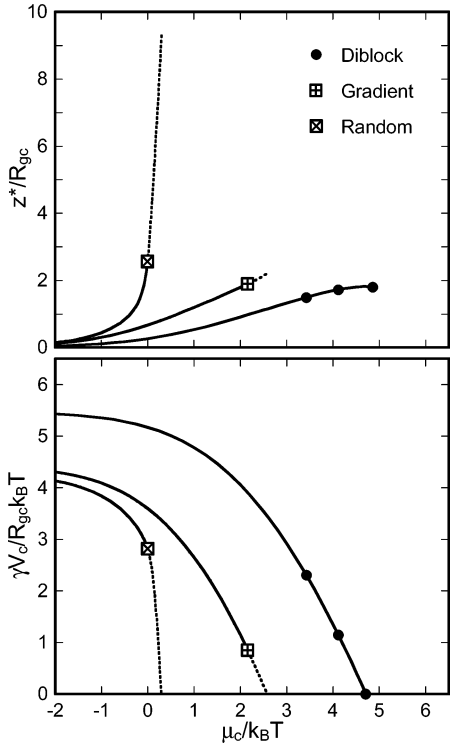

Figure 9. Interfacial excess and interfacial energy as functions of copolymer chemical potential for the diblock, gradient, and random copolymers. The circles are results of the mean-field fits to the FRES data for the diblock copolymer, and the solid lines are calculated by mean-field theory using the value of χ determined by the block copolymer samples, $\chi = 0.036$. The squares correspond to the coexistence points for the random and gradient copolymers, and the dotted lines are extensions of the theory to the point where the interfacial energy is zero.

copolymers cause some of the molecules to have a slightly higher interfacial activity. At higher initial concentrations of copolymer, the number of molecules with a higher interfacial activity is proportionally larger, so the effect is most prominent in the 20% and 30% samples. These variations are particularly important for the random copolymer because the coexistence chemical potential is very close to the wetting transition where the copolymer forms a third layer at the interface. This effect is illustrated in Figure 9.

In Figure 9, the theoretical interfacial excess is plotted for the diblock, gradient, and random copolymers using $\chi = 0.036$, with the three diblock copolymer samples plotted as dark circles. The normalized interfacial energy $\gamma V_c/R_{gc}k_BT$, where γ is the interfacial energy and V_c is the volume of the copolymer ($V_c = v_0N_c$), is also plotted as a function of copolymer chemical potential, also for $\chi = 0.036$. The results for the three diblock copolymer samples are plotted as dark circles, and the end point of the line is where the interfacial energy is zero. The end points (marked by squares) of the random and gradient copolymer lines are at the coexistence points, with dotted lines extending the theory to the point where the interfacial energy is zero. This figure illustrates the important differences in interfacial behavior as λ increases. A divergence in z^*/R_{gc} at the coexistence chemical potential corresponds to the formation of a macroscopic wetting layer at the interface, which is very nearly the situation for the random copolymer ($\lambda = \infty$). Thus, a small variation in chemical potential could result in a large increase in z^*, as seen in the 20% and 30% samples, because the coexistence chemical potential is very close to the wetting transition. For diblock copolymers with $\lambda = 0$, however, the interfacial tension between the phases reaches zero for a relatively small value of z^*/R_{gc}, corresponding to the existence of a single copolymer monolayer at the interface that remains relatively sharp and well-defined. The gradient copolymer with $\lambda = 1$ yields an interface that is intermediate between these two extremes but is similar to the monolayer formed by the diblock. At coexistence, the interfacial energy of the gradient copolymer interface is close to zero. A small variation in chemical potential due to chemical composition and molecular weight distributions similar to the ones seen in the random copolymer would cause the interfacial energy to reach zero, indicating that the copolymer forms a single monolayer at the interface. This also gives us some insight into the behavior seen in the 30% gradient copolymer sample. With an interfacial energy very close to zero, the copolymer may be facilitating the formation of an emulsion phase.

In summary, the diblock, gradient, and random copolymers all have a unique interfacial character, varying from the monolayer of diblock copolymer to the wetting layer of random copolymer. In a gradient copolymer, the parameter λ can be tuned to achieve a desired interfacial excess that is intermediate between the two extremes. The ability to continuously tailor the interfacial width by controlling the sequence distribution has important consequences on a variety of interface properties, including, for example, the interface mechanical toughness.[57]

Conclusions

We have synthesized diblock, random, and gradient copolymers using ROMP. Because the two norbornene-based monomers have reactivity ratios near unity, the gradient copolymer has a linear gradient shape obtained in conjunction with a 50/50 monomer cumulative composition using a dual ramping strategy. The ability to precisely control the composition along the backbone of the chain makes this an ideal model system for studying the interfacial properties of the copolymers. The interfacial segregation of all three copolymers was measured using FRES, and we find that the self-consistent mean-field theory used in this work is a useful tool for describing the copolymer interfacial activity and estimating the degree of incompatibility between the two weakly segregating repeat units. Using the diblock copolymer data, we estimate χ to be 0.036. The gradient parameter, λ, which describes the width of the composition gradient as a fraction of the length of the copolymer chain, can be used to categorize the interfacial behavior of a wide variety of copolymers. For $\lambda = 0$, an adsorbed monolayer is formed at the interface. The maximum copolymer chemical potential in this case is generally limited by the formation of micelles in one of the bulk phases, although for the experimental system investigated here, the thermodynamic interactions were weak enough so that micellization is not expected. Instead, the copolymer continues to adsorb at the interface until the interfacial tension reaches zero in the high-concentration samples. As λ increases toward the limit of ∞ that corresponds to a random copolymer of uniform composition, the thickness of the wetting layer at the interface gradually increases. For sufficiently large values of λ, the maximum copolymer chemical potential

is no longer limited by the formation of micelles but is instead limited by the phase separation of the homopolymer/copolymer blend into disordered copolymer-rich domains within one of the homopolymer phases. The gradient copolymer with $\lambda = 1$ exhibits intermediate behavior, forming a monolayer with low interfacial energy at the interface but with a larger interfacial excess and interfacial width than the monolayer formed by the diblock copolymer. The exact value of λ can be changed to create a tailored interfacial copolymer monolayer that has a desired interfacial width.

Acknowledgment. This work was supported by the MRSEC program of the National Science Foundation (DMR-0520513) at the Materials Research Center of Northwestern University and the MRSEC program (DMR05-20020) at the University of Pennsylvania.

References and Notes

(1) Matyjaszewski, K.; Ziegler, M. J.; Arehart, S. V.; Greszta, D.; Pakula, T. *J. Phys. Org. Chem.* **2000**, *13*, 775.
(2) Matyjaszewski, K.; Xia, J. *Chem. Rev.* **2001**, *101*, 2921.
(3) Davis, K. A.; Matyjaszewski, K. *Adv. Polym. Sci.* **2002**, *159*, 2.
(4) Lutz, J.-F.; Pakula, T.; Matyjaszewski, K. In *Advances in Controlled/Living Radical Polymerization*; Matyjazewski, K., Ed.; American Chemical Society: Washington, DC, 2003; Vol. 854, pp 268−282.
(5) Rizzardo, E.; Chiefari, J.; Chong, B. Y. K.; Ercole, F.; Krstina, J.; Jeffery, J.; Le, T. P. T.; Mayadunne, R. T. A.; Meijs, G. F.; Moad, C. L.; Moad, G.; Thang, S. H. *Macromol. Symp.* **1999**, *143*, 291.
(6) Farcet, C.; Charleux, B.; Pirri, R. *Macromol. Symp.* **2002**, *182*, 249.
(7) Gray, M. K.; Nguyen, S. T.; Zhou, H.; Torkelson, J. M. *Polym. Prepr. (Am. Chem. Soc., Div. Polym. Chem.)* **2002**, *43*, 112.
(8) Gray, M.; Zhou, H.; Nguyen, S. T.; Torkelson, J. M. *Macromolecules* **2004**, *37*, 5586.
(9) Gray, M. Z.; H.; Nguyen, S. T.; Torkelson, J. *Polymer* **2004**, *45*, 4777.
(10) Mignard, E.; Leblanc, T.; Bertin, D.; Guerret, O.; Reed, W. F. *Macromolecules* **2004**, *37*, 966.
(11) Greszta, D.; Matyjaszewski, K. *Polym. Prepr. (Am. Chem. Soc., Div. Polym. Chem.)* **1996**, *37*, 569.
(12) Matyjaszewski, K.; Greszta, D.; Pakula, T. *Polym. Prepr. (Am. Chem. Soc., Div. Polym. Chem.)* **1997**, *38*, 707.
(13) Greszta, D.; Matyjaszewski, K.; Pakula, T. *Polym. Prepr. (Am. Chem. Soc., Div. Polym. Chem.)* **1997**, *38*, 709.
(14) Arehart, S. V.; Matyjaszewski, K. *Macromolecules* **1999**, *32*, 2221.
(15) Ziegler, M. J.; Matyjaszewski, K. *Macromolecules* **2001**, *34*, 415.
(16) Boerner, H. G.; Duran, D.; Matyjaszewski, K.; da Silva, M.; Sheiko, S. S. *Macromolecules* **2002**, *35*, 3387.
(17) Gu, B.; Sen, A. *Macromolecules* **2002**, *35*, 8913.
(18) Qin, S.; Pyun, J.; Saget, J.; Jia, S.; Kowalewski, T.; Matyjaszewski, K. *Polym. Prepr. (Am. Chem. Soc., Div. Polym. Chem.)* **2002**, *43*, 235.
(19) Neugebauer, D.; Matyjaszewski, K. *Polym. Prepr. (Am. Chem. Soc., Div. Polym. Chem.)* **2003**, *44*, 508.
(20) Dettmer, C. M.; Gray, M. K.; Torkelson, J. M.; Nguyen, S. T. *Macromolecules* **2004**, *37*, 5504.
(21) Chojnowski, J.; Cypryk, M.; Fortuniak, W.; Kazmierski, K.; Rozga-Wijas, K.; Scibiorek, M. In *Synthesis and Properties of Silicones and Silicone-Modified Materials*; Clarson, S. J., Ed.; American Chemical Society: Washington, DC, 2003; Vol. 838, pp 12−25.
(22) Jasso, C. F.; Lopez, L. C.; Gonzalez, I. R.; Monsebaiz, D.; Gonzalez-Ortiz, L. J.; Garcia, R. L. H. *Annu. Technol. Conf. Soc. Plast. Eng.* **2002**, *60*, 1640.
(23) Pakula, T. *Macromol. Theory Simul.* **1996**, *5*, 987.
(24) Aksimentiev, A.; Holyst, R. *J. Chem. Phys.* **1999**, *111*, 2329.
(25) Lefebvre, M. D.; Olvera de la Cruz, M.; Shull, K. R. *Macromolecules* **2004**, *37*, 1118.
(26) Shull, K. R. *Macromolecules* **2002**, *35*, 8631.
(27) Pickett, G. T. *J. Chem. Phys.* **2003**, *118*, 3898.
(28) Kim, J.; Gray, M. K.; Zhou, H. Y.; Nguyen, S. T.; Torkelson, J. M. *Macromolecules* **2005**, *38*, 1037.
(29) Brown, H. R.; Char, K.; Deline, V. R.; Green, P. F. *Macromolecules* **1993**, *26*, 4155.
(30) Dai, C.-A.; Dair, B. J.; Dai, K. H.; Ober, C. K.; Kramer, E. J.; Hui, C.-Y.; Jelinski, L. W. *Phys. Rev. Lett.* **1994**, *73*, 2472.
(31) Yeung, C.; Balazs, A. C.; Jasnow, D. *Macromolecules* **1992**, *25*, 1357.
(32) Faldi, A.; Genzer, J.; Composto, R. J.; Dozier, W. D. *Phys. Rev. Lett.* **1995**, *74*, 3388.
(33) Lee, M. S.; Lodge, T. P.; Macosko, C. W. *J. Polym. Sci., Part B: Polym. Phys.* **1997**, *35*, 2835.
(34) Genzer, J.; Composto, R. J. *Macromolecules* **1998**, *31*, 870.
(35) Lyatskaya, Y.; Gersappe, D.; Gross, N. A.; Balazs, A. C. *J. Phys. Chem.* **1996**, *100*, 1449.
(36) Adedeji, A.; Lyu, S.; Macosko, C. W. *Macromolecules* **2001**, *34*, 8663.
(37) Sundararaj, U.; Macosko, C. W. *Macromolecules* **1995**, *28*, 2647.
(38) Shull, K. R.; Kramer, E. J. *Macromolecules* **1990**, *23*, 4769.
(39) Shull, K. R.; Kramer, E. J.; Hadziioannou, G.; Tang, W. *Macromolecules* **1990**, *23*, 4780.
(40) Fredrickson, G. H.; Milner, S. T.; Leibler, L. *Macromolecules* **1992**, *25*, 6341.
(41) Shakhnovich, E. I.; Gutin, A. M. *J. Phys. (Paris)* **1989**, *50*, 1843.
(42) Sfatos, C. D.; Gutin, A. M.; Shakhnovich, E. I. *Phys. Rev. E* **1993**, *48*, 465.
(43) Gersappe, D.; Balazs, A. C. *Phys. Rev. E* **1995**, *52*, 5061.
(44) Pangborn, A. B.; Giardello, M. A.; Grubbs, R. H.; Rosen, R. K.; Timmers, F. J. *Organometallics* **1996**, *15*, 1518.
(45) Meddour, A.; Courtieu, J. *Tetrahedron: Asymmetry* **2000**, *11*, 3635.
(46) Pedersen, A. K.; FitzGerald, G. A. *J. Pharm. Sci.* **1985**, *74*, 188.
(47) Wu, Z.; Nguyen, S. T.; Grubbs, R. H.; Ziller, J. W. *J. Am. Chem. Soc.* **1995**, *117*, 5503.
(48) Drouin, S. D.; Zamanian, F.; Fogg, D. E. *Organometallics* **2001**, *20*, 5495.
(49) Composto, R. J.; Walters, R. M.; Genzer, J. *Mater. Sci. Eng. R* **2002**, *38*, 107.
(50) Matsen, M. W. *J. Phys.: Condens. Matter* **2002**, *14*, R21.
(51) van Lent, B.; Scheutjens, J. M. H. M. *J. Phys. Chem.* **1990**, *94*, 5033.
(52) Chen, Z. Y. *J. Chem. Phys.* **2000**, *112*, 8665.
(53) Shi, T. F.; Ziegler, V. E.; Welge, I. C.; An, L. J.; Wolf, B. A. *Macromolecules* **2004**, *37*, 1591.
(54) Sides, S. W.; Fredrickson, G. H. *J. Chem. Phys.* **2004**, *121*, 4974.
(55) Stockmayer, W. H. *J. Chem. Phys.* **1945**, *13*, 199.
(56) Soares, J. B. P.; Monrabal, B.; Nieto, J.; Blanco, J. *Macromol. Chem. Phys.* **1998**, *199*, 1917.
(57) Creton, C.; Kramer, E. J.; Brown, H. R.; Hui, C.-Y. *Adv. Polym. Sci.* **2002**, *156*, 53.

MA0509762